

ARTICLES

Differential cross sections of J/ψ and ψ' in 800 GeV/c p -Si interactions

T. Alexopoulos,¹ L. Antoniazzi,² M. Arenton,³ H. C. Ballagh,⁴ H. Bingham,⁴ A. Blankman,⁵ M. Block,⁶ A. Boden,⁷ G. Bonomi,² Z. L. Cao,³ T. Y. Chen,⁸ K. Clark,⁹ D. Cline,⁷ S. Conetti,³ M. Cooper,¹⁰ G. Corti,³ B. Cox,³ P. Creti,¹¹ C. Dukes,³ C. Durandet,¹ V. Elia,¹¹ A. R. Erwin,¹ L. Fortney,¹² V. Golovatyuk,¹¹ E. Gorini,¹¹ F. Grancagnolo,¹¹ K. Hagan-Ingram,³ M. Haire,¹³ P. Hanlet,³ M. He,¹⁴ G. Introzzi,² M. Jenkins,⁹ D. Judd,¹³ W. Kononenko,⁵ W. Kowald,¹² K. Lau,¹⁵ A. Ledovskoy,³ G. Liguori,² J. Lys,⁴ P. O. Mazur,¹⁶ A. McManus,³ S. Misawa,⁴ G. H. Mo,¹⁵ C. T. Murphy,¹⁶ K. Nelson,³ M. Panareo,¹¹ V. Pogosian,³ S. Ramachandran,⁷ J. Rhoades,⁷ W. Selove,⁵ R. P. Smith,¹⁶ L. Spiegel,¹⁶ J. G. Sun,³ S. Tokar,¹⁷ P. Torre,² J. Trischuk,¹⁸ L. Turnbull,¹³ D. E. Wagoner,¹³ C. R. Wang,¹⁴ C. Wei,¹² W. Yang,¹⁶ N. Yao,⁸ N. J. Zhang,¹⁴ and B. T. Zou¹²

¹University of Wisconsin, Madison, Wisconsin 53706

²University and INFN of Pavia, Pavia, Italy

³University of Virginia, Charlottesville, Virginia 22901

⁴University of California at Berkeley, Berkeley, California 94720

⁵University of Pennsylvania, Philadelphia, Pennsylvania 19104

⁶Northwestern University, Evanston, Illinois 60208

⁷University of California at Los Angeles, Los Angeles, California 90024

⁸Nanjing University, Nanjing, People's Republic of China

⁹University of South Alabama, Mobile, Alabama 36688

¹⁰Vanier College, Montreal, Quebec, Canada H4L 3X9

¹¹University and INFN of Lecce, Lecce, Italy

¹²Duke University, Durham, North Carolina 27706

¹³Prairie View A&M, Prairie View, Texas 77446

¹⁴Shandong University, Jinan, Shandong, People's Republic of China

¹⁵University of Houston, Houston, Texas 77204

¹⁶Fermilab, Batavia, Illinois 60510

¹⁷Comenius University, Bratislava, Slovakia

¹⁸McGill University, Montreal, Quebec, Canada H3A 2T8

(Received 30 July 1996)

We present the x_F and p_T differential cross sections of J/ψ and ψ' , respectively, in the ranges $-0.05 < x_F < 0.25$ and $p_T < 3.5$ GeV/c. The data samples are constituted by about 12 000 J/ψ and 200 ψ' produced in proton-silicon interactions at 800 GeV/c and decaying into opposite sign muons. The x_F and p_T distributions are compared with recent results from experiments E789 at the same energy and to leading order QCD predictions using the MRS D0 parametrization for the parton structure function. The measured shapes of the differential cross sections, except for the $d\sigma/dx_F$ at small x_F , agree very well with the prediction, even though their value is quite a bit larger than the prediction. We also present the $\cos\theta$ differential cross section of the J/ψ which indicates unpolarized production in contrast with color octet models predictions. [S0556-2821(97)01605-6]

PACS number(s): 13.85.Ni, 13.60.Le

I. INTRODUCTION

Hadronic production of charmonium states is one of the most studied processes in high energy physics. In spite of this experimental effort, the mechanisms of quarkonium production are not well understood, and calculations of higher order contributions are still missing. In addition, the formation of the $c\bar{c}$ bound states is a nonperturbative QCD process and requires some understanding of the evolution from the quark-antiquark color octet to the physical quarkonium states. The renewed interest in these subjects, owing to Tevatron collider results [3], has led to a better theoretical understanding of these mechanisms with the development of a new

model in the past couple of years [1,2]. One of the features of this model is that it predicts high transverse polarization of quarkonium states.

The study of inclusive J/ψ production is complicated by additional contributions from radiative decays of higher-mass states ($\chi_{i=0,1,2}$ and ψ') to the direct production, making comparison with theory more difficult. In this paper we report on the x_F and p_T differential cross sections for J/ψ and ψ' in the ranges $-0.05 < x_F < 0.25$ and $p_T < 3.5$ GeV/c. We compare these cross sections with the recent published results of experiment E789 [4] obtained at the same energy, and with leading order QCD calculations using Martin-Roberts-Stirling (MRS) [5] parton distributions. We

also report on measurement of the differential angular distribution of the J/ψ and compare this to the color octet predictions.

II. EXPERIMENTAL SETUP

A. Beam and target

The data were collected at the High Intensity Laboratory in a primary proton beam at Fermilab with the E771 spectrometer during a short run of 5 weeks.

The 800 GeV/c beam, of average intensity $\approx 4 \times 10^7$ proton/s per 23 s spill every 57 s, interacted with a silicon target consisting of 12 foils, each 2 mm thick and spaced 4 mm apart, for a total of 5.3% of an interaction length. The resulting average interaction rate was approximately 2 MHz.

The beam was monitored by means of an ion chamber and beam silicon strip detectors placed along the beam line, which gave a total integrated number of live protons on target of 1.313×10^{13} with an error of approximately 5% dominated by the uncertainty in the efficiency of the beam silicon detector.

B. Spectrometer

The E771 spectrometer [6,7] was optimized for the observation of dimuons coming from J/ψ 's generated in the decays of heavy quark states. It consisted of a silicon microstrip detector, a tracking section upstream and downstream of an analysis magnet, an electromagnetic calorimeter, and a muon detector placed after a hadron absorber. Neither the microstrip detector nor the calorimeter was used for the analysis described here.

The tracking section consisted of 22 planes of multiwire proportional chambers (MWPC's), 9 planes of drift chambers to define the charged particle trajectories upstream of the analysis magnet, 12 planes of drift, and 6 of drift-pad [8] chambers downstream of the magnet. All chambers are dead-ended in a region around the beam axis with a resulting minimum acceptance angle of 25 mrad. The analysis magnet, a

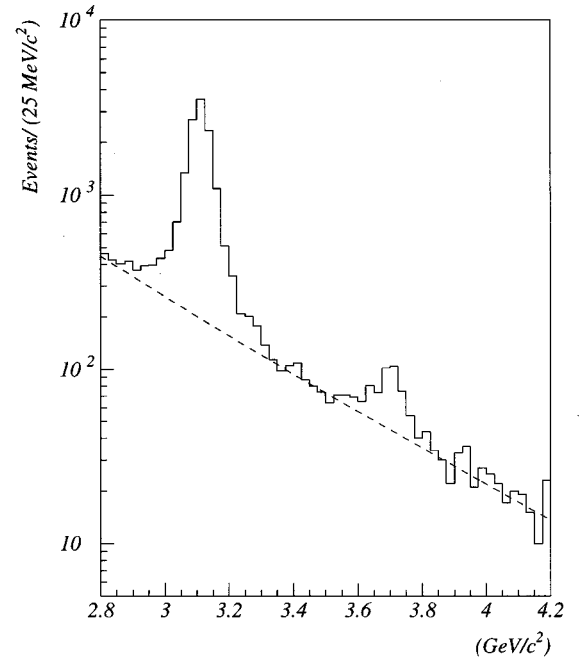


FIG. 1. Invariant mass spectrum of the $\mu^+ \mu^-$ pairs. The dashed line is the continuum background as described in the text.

dipole with 185×90 cm² aperture, provided a p_T kick of 0.82 GeV/c in the horizontal plane.

The muon detector, located downstream of a 3 m thick hadron absorber, made of steel (copper in the central part), consisted of three planes of resistive plate counters (RPC's) and three planes of scintillators separated by steel, concrete, and lead absorbers. The RPC's are thin gap (2 mm) gas devices operating in the streamer mode under a high uniform electric field (40 kV/cm). The charge produced by the streamer process is picked up by external copper pads [9].

The single and dimuon triggers, entirely based on the RPC signals, define a muon as the triple coincidence among a projective set of pads belonging to the three RPC planes [10,11]. The minimum momentum required for a muon to

TABLE I. J/ψ cross section for each bin of x_F and p_T . There is an overall systematic error of 8%.

x_F bin range	$d\sigma/dx_F$ (nb/nucleon)	p_T bin range (GeV/c)	$d\sigma/dp_T^2$ [nb(GeV/c) ⁻² /nucleon]
-0.05--0.03	1309 ± 78	0.0-0.3	197 ± 17
-0.03--0.01	1352 ± 70	0.3-0.6	175.9 ± 9.8
-0.01-0.01	1327 ± 56	0.6-0.9	134.9 ± 5.9
0.01-0.03	1242 ± 48	0.9-1.2	101.1 ± 4.2
0.03-0.05	1134 ± 44	1.2-1.5	64.7 ± 2.8
0.05-0.07	963 ± 46	1.5-1.8	41.5 ± 2.3
0.07-0.09	776 ± 35	1.8-2.1	22.6 ± 1.6
0.09-0.11	701 ± 36	2.1-2.4	12.3 ± 1.4
0.11-0.13	591 ± 35	2.4-2.8	4.8 ± 0.5
0.13-0.15	508 ± 34	2.8-3.2	1.84 ± 0.27
0.15-0.17	463 ± 39	3.2-3.6	0.59 ± 0.20
0.17-0.19	427 ± 38		
0.19-0.21	353 ± 40		
0.21-0.23	254 ± 28		
0.23-0.25	294 ± 39		

TABLE II. ψ' cross section for each bin of x_F and p_T . There is an overall systematic error of 23%.

x_F bin range	$d\sigma/dx_F$ (nb/nucleon)	p_T bin range (GeV/c)	$d\sigma/dp_T^2$ [nb(GeV/c) $^{-2}$ /nucleon]
-0.06--0.02	148±59	0.0-0.4	25.1±8.0
-0.02-0.02	199±45	0.4-0.7	23.3±5.4
0.02-0.06	127±30	0.7-1.0	15.3±4.0
0.06-0.10	82±25	1.0-1.4	13.6±2.2
0.10-0.14	87±18	1.4-2.4	2.4±0.7
0.14-0.18	54±12	2.4-3.4	0.51±0.26
0.18-0.22	37±17		
0.22-0.26	32±13		

penetrate the absorbers and produce a signal in the third RPC plane is 10 GeV/c in the central part and about 6 GeV/c at wider angles.

Further details of the E771 spectrometer can be found elsewhere [7].

III. DATA ANALYSIS

The collected data amounted to about 130 million dimuon triggers and 60 million single-muon triggers recorded on 1200 exabyte cassette tapes. The 130 million dimuon trigger events were processed with a fast filter program which, starting from muon candidates, defined as the coincidence of at least 4 out of the 3 RPC and 3 scintillator planes, reconstructed only the muon tracks downstream of the analysis magnet. In the subsequent analysis, these muons were fully tracked in all chambers and through the analysis magnet. Opposite sign dimuons, constrained to a common vertex, were selected. Only the pair with the best vertex constrained fit χ^2 was considered for this analysis.

The overall reconstruction efficiencies and acceptances were obtained by generating about 10^6 Monte Carlo (MC) events for the J/ψ and 10^5 for the ψ' . The first iteration differential distributions used in the MC were taken from earlier experiments at lower energy. The mesons were assumed to decay isotropically. The decay muons were propagated through a GEANT simulation of the E771 detector taking into account the measured chamber and trigger efficiencies [9–11] and the contribution of multiple scattering. To simulate realistic noise in the detector, the generated events were superimposed on real events. In the high-end x_F bins, the distribution of reconstructed masses was fit with two Gaussians while the mass distribution on the midrange bins was fit with three Gaussians. In the latter case the widest

Gaussians was considered as background because an independent study showed that events in the wider Gaussian were primarily cases in which the reconstructed x_F was more than 3σ different than the generated ones. The ranges of x_F and p_T over which the experiment is sensitive are, respectively, $-0.05 < x_F < 0.25$ and $p_T < 3.5$ GeV/c. The average relative resolutions are 6.0% in x_F and 6.7% in p_T . The range for the angular distribution is $-0.8 < \cos\theta < 0.8$.

IV. EXPERIMENTAL RESULTS

Figure 1 shows the invariant mass spectrum of the selected opposite sign dimuons. A total of $11\,660 \pm 139 J/\psi$ and $218 \pm 24 \psi'$ are obtained from fits to the background subtracted number of events in the two peaks. The dashed line represents the background, fitted to the function

$$\frac{a}{m_{\mu\mu}^3} \exp(-bm_{\mu\mu}) \quad , \quad (1)$$

which is mainly due to muons from π and K decays, to the Drell-Yan process and to charm production. Contributions from B mesons are negligible.

The mass resolution of the spectrometer depends on x_F , ranging from 20 MeV/c² at $x_F = -0.05$ to about 100 MeV/c² at $x_F = 0.25$, while it is totally independent of the transverse momentum, in agreement with Monte Carlo simulation.

The differential distributions have been extracted by fitting the mass spectra in each of the x_F and p_T bins with the resolution functions of the two resonances (the sum of two Gaussians for the J/ψ and a single Gaussian for the ψ') over the described background. The use of two Gaussians for the

TABLE III. Results of the fits performed on the differential distributions as described in the text.

Meson	Function	A	n	χ^2/DOF
J/ψ	$A(1 - x_F)^n$	1424±31 nb	6.54±0.23	1.65
J/ψ	$A(1 - x_F)^n$	1386±33 nb	6.38±0.24	0.92
ψ'	$A(1 - x_F)^n$	178±29 nb	6.7±1.3	0.24
ψ'	$A(1 - x_F)^n$	172±17 nb	6.38(fixed)	0.26
J/ψ	$A \exp(-np_T^2)$	182±5 nb(GeV/c) $^{-2}$	0.54±0.01 (GeV/c) $^{-2}$	0.93
J/ψ	$A \exp(-np_T^2)$	185±5 nb(GeV/c) $^{-2}$	0.55±0.01 (GeV/c) $^{-2}$	0.60
ψ'	$A \exp(-np_T^2)$	27±4 nb(GeV/c) $^{-2}$	0.61±0.08 (GeV/c) $^{-2}$	1.02

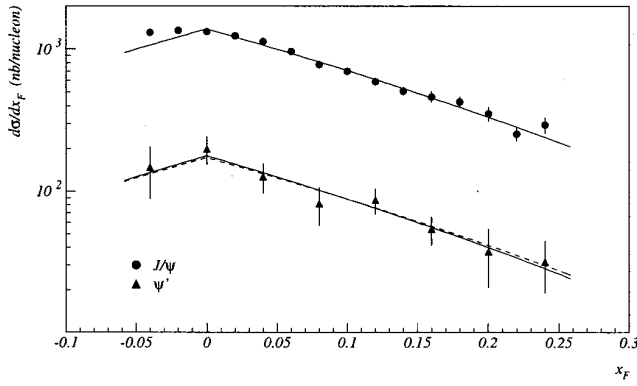


FIG. 2. Differential cross sections for J/ψ and ψ' vs x_F . The 8% (J/ψ) and 23% (ψ') systematic uncertainties due to the normalization are not shown. Superimposed on the data are the fits described in the text. The dashed line is a fit to the ψ' data with the exponential parameter fixed to the corresponding value for J/ψ .

J/ψ , suggested by Monte Carlo studies, is motivated by the different quality of the information obtainable in highly populated hit regions.

In order to minimize systematics, the procedure for extracting the differential distribution was iterated by inserting into the Monte Carlo the extracted x_F and p_T distributions, corrected for the resulting acceptances and efficiencies, until convergence and stability of the result was reached.

The differential cross sections have been computed by assuming an atomic weight dependence A^α , with $\alpha = 0.920 \pm 0.008$ [12]. The choice of this value is justified by the adequate description of the available data [12] for a silicon target ($A = 28$) and, because in our range of x_F and p_T , α appears to be fairly constant [12,13]. The values of the branching ratios $B(J/\psi \rightarrow \mu^+ \mu^-)$ and $B(\psi' \rightarrow \mu^+ \mu^-)$ have been taken from Ref. [14].

The measured differential cross sections for each of the x_F and p_T bins are listed in Table I for the J/ψ and in Table II for the ψ' . In addition to the errors shown there are overall systematic uncertainties of 8% for the J/ψ and 23% for the ψ' , due to the uncertainties in luminosity, branching ratios, and acceptance.

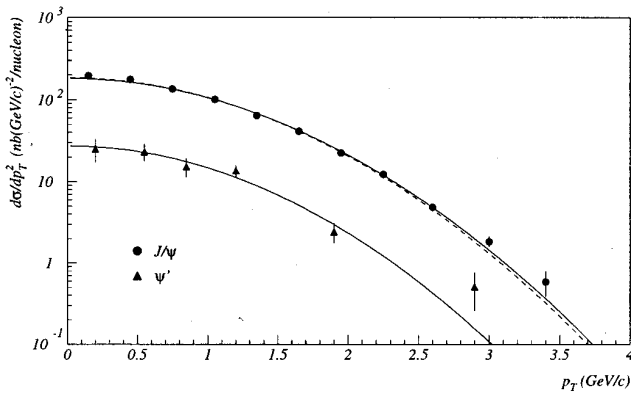


FIG. 3. Differential cross sections for J/ψ and ψ' vs p_T . The 8% (J/ψ) and 23% (ψ') systematic uncertainties due to the normalization are not shown. Superimposed on the data are the fits described in the text. The dashed line is a fit to the J/ψ data performed by excluding the last two points.

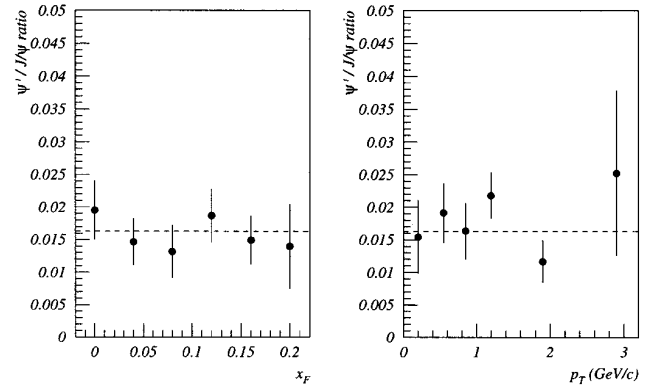


FIG. 4. Ratio $B(\psi' \rightarrow \mu^+ \mu^-) \times \sigma(\psi')$ to $B(J/\psi \rightarrow \mu^+ \mu^-) \times \sigma(J/\psi)$ vs x_F and p_T .

The $d\sigma/dx_F$ cross sections per nucleon are shown in Fig. 2 as a function of the fractional longitudinal momentum x_F of the J/ψ and ψ' . The data have been fit with an empirical function of the form

$$\frac{d\sigma}{dx_F} = A(1 - |x_F|)^n. \quad (2)$$

The fit parameters are shown in Table III. The first row in the table shows the results of a fit to all the data points, while the second row (corresponding to the line fit of Fig. 2) shows the fit excluding the two negative x_F values. The fourth row in Table III lists the fit parameters for ψ' when n is forced to be equal to the corresponding value of the J/ψ fit.

Analogously, the $d\sigma/dp_T^2$ cross sections per nucleon versus the transverse momentum of the produced meson, for both charmonium states, are shown in Fig. 3. The data were parametrized by

$$\frac{d\sigma}{dp_T^2} = A \exp(-np_T^2). \quad (3)$$

Again, the fit parameters are listed in Table III. The fifth row in the table shows the results of a fit to all data points. The fit for the J/ψ has been also performed by excluding the last two points in order to directly compare our result to the one

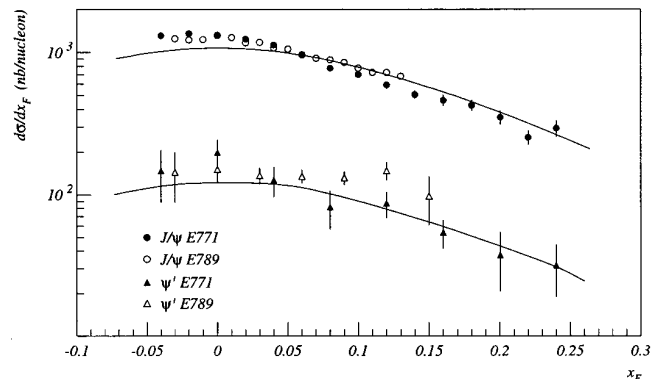


FIG. 5. E771 differential cross sections for J/ψ and ψ' vs x_F compared with the E789 results and with MRSD0 theoretical predictions, arbitrarily normalized to E771 data.

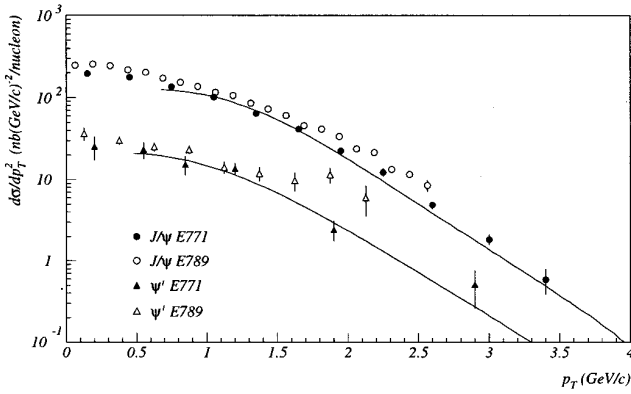


FIG. 6. E771 differential cross sections vs p_T compared with the E789 results and with MRSD0 theoretical predictions, arbitrarily normalized to E771 data.

of Fermilab E789 [4] where a smaller range of p_T is used. The parameters of this fit are listed in the sixth row of Table III.

It is worth noticing that, within experimental errors, both differential cross sections for the two charmonium states are described by the same parameters, suggesting that they are produced by the same mechanisms. In fact, Fig. 4 shows that there is no evident dependence on x_F and p_T of the ratio:

$$\frac{B(\psi' \rightarrow \mu^+ \mu^-) \sigma(\psi')}{B(J/\psi \rightarrow \mu^+ \mu^-) \sigma(J/\psi)} \quad (4)$$

in which the uncertainties in the absolute normalization and the systematics arising from the knowledge of the branching ratios cancel out. These results seem to disagree with recently published data at same energy [4] where a mild increase in this ratio with x_F and p_T is reported.

In Fig. 5 and Fig. 6 we compare our x_F and p_T distributions for the J/ψ and ψ' with those of Fermilab E789 [4]. The cross sections of the two experiments differ by an overall scale factor because of a different choice of the parameter α (E789 uses $\alpha=0.9$, instead of $\alpha=0.92$ which gives a difference of about 11% for the E789 target with $A=197$).

While the shapes of $d\sigma/dp_T^2$ are in very good agreement, the x_F distributions show some discrepancy ($n_{E789}=4.91 \pm 0.18$, $n_{E771}=6.38 \pm 0.24$). The nature of this inconsistency is unknown. Nuclear effects due to the very different atomic weights of the target [12] would predict an even larger difference in the value of n , though, in this range of x_F , as already pointed out, the value of α can be assumed constant.

In Fig. 5 and Fig. 6 we compare also our results to the theoretical predictions [15] computed using perturbative QCD to leading order for both differential distributions of the two charmonium states. These predictions are still based on the color singlet model [16], because the differential distribution for the most advanced model developed in the last years, the color octet mechanism [1], are not yet available at low p_T . The contributions of various quarkonium states to the inclusive J/ψ cross section are taken into account by using the known branching ratio of the $\chi_{0,1,2}$ and ψ' states

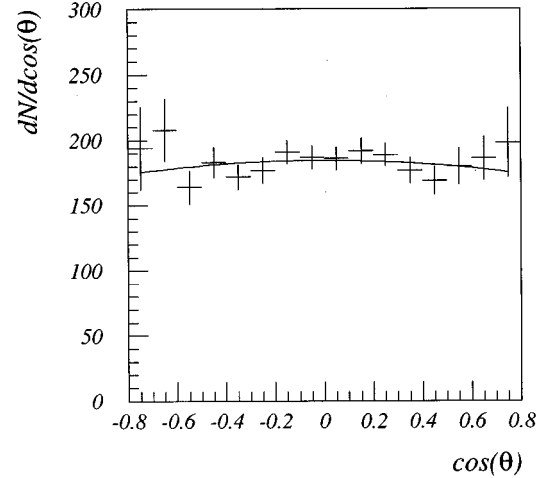


FIG. 7. $\cos\theta$ differential cross section. Superimposed on the data is the fit described in the text.

decaying in J/ψ [14]. The Martin-Roberts-Stirling set D0 (MRS D0) [5] for the parton structure function has been used for comparison with our data.

Both the shapes and the scale of the theoretical predictions disagree with our data for the $d\sigma/dx_F$ cross sections. The K factors needed to normalize the curves are $K \approx 4$ for J/ψ and $K \approx 16$ for ψ' while the disagreement in shape is mainly at small x_F .

The shape of $d\sigma/dp_T^2$ cross sections is in good agreement with our data, but still needs a scale factor for the normalization. In this case $K \approx 9$ for J/ψ , while for ψ' $K \approx 14$ needs to be used. These $d\sigma/dp_T^2$ predictions are obtained by assuming an intrinsic p_T Gaussian distribution for the partons with $\langle p_T^2 \rangle = 0.5 \text{ (GeV/c)}^2$. To eliminate the divergences at low p_T due to χ_0 and χ_2 states we had to apply an arbitrary cutoff at 0.6 GeV/c for the J/ψ and at 0.4 GeV/c for the ψ' . In fact, the listed K factors depends strongly on the choice of this cut and therefore are experiment dependent.

We also computed the total cross sections for J/ψ and ψ' . Assuming that Eq. (2) describes all the x_F range, we get $\sigma(J/\psi) = 375 \pm 4 \pm 30 \text{ nb}$ and $\sigma(\psi') = 46 \pm 3 \pm 10 \text{ nb}$. These values are consistent with those obtained in a previous analysis [17] and with a recent computation of the total cross section using the color octet model [2].

Finally the same procedure was used to obtain the $d\sigma/d\cos\theta$ differential cross section shown in Fig. 7. The angle θ is defined as the angle between the positive muon and beam direction in the J/ψ rest frame. In this case the fit has been performed with the function $A(1 + \alpha\cos^2\theta)$ obtaining $\alpha = -0.09 \pm 0.12$. This result is in disagreement with the color octet model [2] which predicts a sizable J/ψ transverse polarization, emphasizing the need for the inclusion of higher twists terms in the description of quarkonium production.

ACKNOWLEDGMENTS

We thank M. L. Mangano for his support and the discussions about the QCD theoretical distributions. We acknowledge the invaluable help of the Fermilab staff including the

Research and Computing Division personnel. This work was supported by the U.S. Department of Energy, the National Science Foundation, the Natural Science and Engineering

Research Council of Canada, the Istituto Nazionale di Fisica Nucleare of Italy, and the Texas Advanced Research Program.

-
- [1] E. Braaten and S. Fleming, *Phys. Rev. Lett.* **74**, 3327 (1995); P. Cho and A. K. Leibovich, *Phys. Rev. D* **53**, 150 (1996).
- [2] M. Beneke and I. Z. Rothstein, *Phys. Rev. D* **54**, 2005 (1996); **54**, 7082(E) (1996).
- [3] CDF Collaboration, F. Abe *et al.*, Fermilab Report No. Fermilab-Conf-94/136 (unpublished); F. Abe *et al.*, Fermilab Report No. Fermilab-Conf-95/128 (unpublished).
- [4] M. H. Schub *et al.*, *Phys. Rev. D* **52**, 1307 (1995).
- [5] A. D. Martin, W. J. Stirling, and R. G. Roberts, *Phys. Lett. B* **306**, 145 (1993).
- [6] T. Alexopoulos *et al.*, *Nucl. Phys.* **B27**, 257 (1992).
- [7] T. Alexopoulos *et al.*, *Nucl. Instrum. Methods Phys. Res. A* **376**, 375 (1996).
- [8] L. Spiegel *et al.*, Fermilab Report No. FERMILAB-TM-1765, 1991 (unpublished).
- [9] G. Cataldi *et al.*, *Nucl. Instrum. Methods Phys. Res. A* **337**, 350 (1994).
- [10] L. Antoniazzi *et al.*, *Nucl. Instrum. Methods Phys. Res. A* **355**, 320 (1995).
- [11] L. Antoniazzi *et al.*, *Nucl. Instrum. Methods Phys. Res. A* **360**, 334 (1995).
- [12] M. R. Alde *et al.*, *Phys. Rev. Lett.* **66**, 133 (1991).
- [13] M. J. Leitch *et al.*, *Phys. Rev. D* **52**, 4251 (1995).
- [14] Particle Data Group, L. Montanet *et al.*, *Phys. Rev. D* **50**, 1173 (1994).
- [15] M. L. Mangano (private communication); “Quarkonium Productions Codes” report (unpublished).
- [16] E. L. Berger and D. Jones, *Phys. Rev. D* **23**, 1521 (1981); B. Guberina *et al.*, *Nucl. Phys.* **B174**, 317 (1981); R. Bayer and R. Rückl, *Z. Phys. C* **19**, 251 (1983); B. Humbert, *Phys. Lett. B* **184**, 105 (1987); R. Gastmans *et al.*, *Nucl. Phys.* **B291**, 731 (1987).
- [17] T. Alexopoulos *et al.*, *Phys. Lett. B* **374**, 271 (1996).